

# Jet coherence in QCD media: the antenna radiation spectrum

Yacine Mehtar-Tani<sup>a</sup>, Konrad Tywoniuk<sup>b</sup>

<sup>a</sup> *Departamento de Física de Partículas and IGFAE, Universidade de Santiago de Compostela, E-15 782 Santiago de Compostela, Galicia-Spain*

<sup>b</sup> *Department of Astronomy and Theoretical Physics, Lund University, Sölvegatan 14A, SE-22 362 Lund, Sweden*

---

## Abstract

We study the radiation pattern of a highly energetic partonic antenna in a colored state traversing a dense QCD medium. Resumming multiple scatterings of all involved constituents with the medium we derive the general gluon spectrum which encompasses both longitudinal color coherence between scattering centers in the medium, responsible for the well known Landau-Pomeranchuk-Migdal (LPM) effect, and transverse color coherence between partons inside a jet, leading, in vacuum, to angular ordering of the parton shower. We identify the relevant scales of the problem and show the emergence of an extended window where transverse coherence is at work for dense media leading to gradual decoherence of the antenna. This naturally restricts the regime of incoherent medium-induced radiation to small-angles (in-cone) and high gluon energies. It follows that in the totally opaque limit the partons *decohere* and radiate independently *as if* in vacuum.

*Keywords:* pQCD, Jets, Heavy Ion Collisions, Jet-Quenching

---

PACS numbers: 12.38.-t, 24.85.+p, 25.75.-q

## 1. Introduction

One of the key objectives of the heavy-ion program at the LHC is to investigate properties of the quark-gluon plasma (QGP) using hard probes. Typically, one addresses modifications of the fragmentation properties of final state energetic particles in medium that depart from the well-known fragmentation pattern in vacuum, e.g., in  $e^+e^-$  annihilation, proton-proton collisions, etc., where no medium is formed. These modifications are assumed to be sensitive to local medium properties, such as the density, as well as their spatiotemporal evolution. Indeed, strong medium effects are observed in heavy-ion collisions for

---

*Email addresses:* mehtar@fpaxp1.usc.es (Yacine Mehtar-Tani),  
konrad.tywoniuk@thep.lu.se (Konrad Tywoniuk)

both single-inclusive leading particle spectra [1, 2, 3] and two-particle correlations [4, 5]. While such measurements have reached a high level of sophistication, shedding light on qualitative aspects of the quark-gluon plasma, studies of intrajet distributions in heavy ion collisions have only recently been initiated both at RHIC [6, 7, 8] and LHC [9, 10] with many promising results and prospects for the future.

The increased experimental capabilities at these high energies have also triggered several efforts to improve the theoretical understanding of gluon radiation in the presence of a colored medium. Until recently, only the leading order one-gluon medium-induced emission spectrum off a highly energetic quark or gluon, that measures radiative parton energy loss in the QGP, which will be denoted BDMPS-Z throughout this work, was known [11, 12, 13, 14]. An equivalent formulation has also been derived in [15, 16, 17, 18]. In particular, this spectrum accounts for momentum broadening of the gluon which undergoes multiple scattering with the medium. Regrettably, since the process under consideration does not encompass interference effects between emitters, see Section 2, the extension to multi-gluon emissions is bound to rely on *ad hoc* conjectures.

To study the importance of these radiative interferences, lately, we calculated the gluon emission spectrum off a time-like quark-antiquark ( $q\bar{q}$ ) antenna. In [19] we considered the situation of a singlet antenna traversing a relatively thin medium, i.e., assuming only one scattering with medium background potential. In [20], on the other hand, we resummed multiple scatterings in the limit of soft gluon emission. The aim of the present work is to generalize the latter results to arbitrary number of rescatterings of the quark, antiquark and gluon, thus extending the validity of our previous results to arbitrarily opaque media and up to large gluon energies. Additionally, we aim at addressing some of the striking features observed in [19, 20] analytically, thus further deepening our understanding of the physical picture at hand.

In vacuum, the antenna spectrum provides a simple laboratory incorporating the basic features of QCD color coherence [21, 22, 23]. Namely, in addition to the typical double-logarithmic structure of vacuum radiation one finds that the phase space of emissions is restricted by angular ordering [24, 25]. While the BDMPS-Z spectrum off a single emitter is infrared and collinear safe due to destructive interference for soft and collinear gluons, we have found that the medium-induced antenna spectrum diverges in the soft limit [19]. Furthermore, up to sizable gluon energies there is a strict angular separation between vacuum and medium-induced radiation leading to a partial decoherence of the total gluon spectrum controlled by medium properties [20]. It is of great importance to see how these features arise in the most general case of multiple scattering. Specifically, it allows to go to the limit of opaque media in a well controlled way.

Finally, we anticipate the importance of the antenna spectrum, which has proven to be the fundamental building block of the QCD vacuum cascade, for the future efforts to establish a jet calculus in medium.

The paper is structured as follows. At the outset, in Section 2, we discuss briefly the known coherence phenomena relevant for high-energy physics and heavy-ion collisions. Then, in Section 3, we present and solve the classical

Yang-Mills equations for the  $q\bar{q}$  antenna, thus obtaining the induced gluon field from multiple scatterings with the medium. Medium averages for the total spectrum are described in Section 4, where we also present the main result of this work, namely the interference spectrum  $\mathcal{J}$  in (36). The general properties of this spectrum are also outlined in some detail. In particular, the emergence of strong color screening leading to a “memory loss” effect in the limit of opaque media is described in Section 5. In Section 6, we outline the main features of in-medium coherence. In particular, we identify three scales that consistently map out the regimes of coherent and incoherent medium-induced radiation. We demonstrate that a large medium density significantly reduces the phase space for incoherent BDMPS-Z radiation. Finally, we summarize and conclude in Section 7.

## 2. Color coherence phenomena in a few words

Coherence phenomena in jet physics have been extensively studied in the framework of perturbative QCD since the early 80’s (see, e.g., [21, 22, 27] and references therein). It has been shown that they substantially affect experimental observables. The effect that proved to be crucial dealt with jet evolution in vacuum: the so called color coherence inside a jet. The cascading of a jet, initiated by a hard parton, occurs in a coherent manner. In other words, parton branchings inside the shower are not independent but depend on the branching of the parent partons, i.e., as a Markovian process. More precisely, it was found that successive parton branchings are ordered in angles thus limiting the phase space for soft emissions that tend to occur at large angles. Experimentally, this fact is manifested in the depletion of soft hadrons in the single-inclusive particle distribution, which exhibits the so-called humpbacked plateau.

The feature of angular ordering reflects the transverse dynamics of the jet. As a simple example, let us consider the radiation pattern off a  $q\bar{q}$  antenna with opening angle  $\theta_{q\bar{q}}$  in a color singlet state. As long as the transverse wave length of the radiated gluon  $\lambda_{\perp} \sim 1/k_{\perp}$  is smaller than the transverse dipole separation when the gluon is formed  $r_{\perp} \sim t_{\text{form}}\theta_{q\bar{q}}$  (the formation time being defined as  $t_{\text{form}} \sim \omega/k_{\perp}^2$  where  $\omega$  and  $k_{\perp}$  are the gluon energy and transverse momentum, respectively), the gluon resolves the color structure of the pair and therefore is radiated either off the quark or the antiquark. In the opposite case the radiation is strongly suppressed since the gluon cannot resolve the color structure of the antenna. Translated in terms of angles, gluons emitted at angles  $\theta > \theta_{q\bar{q}}$  are suppressed. Clearly, this coherence phenomenon arises as long as two or more emitting particles are involved. In general, small-angle radiation which resolves the independent emitters is incoherent while large-angle gluons are sensitive to the charge of the whole system and are therefore emitted coherently. In the following we shall refer to this color coherence phenomenon by “transverse coherence”.

In the case of a medium, another type of coherence arises which we, in contrast to the above, will call “longitudinal coherence”. Namely, when the medium is dense enough an energetic particle can scatter coherently off several

scattering centers along its trajectory during its formation time,  $t_{\text{form}} \sim N_{\text{coh}}\lambda$  ( $\lambda$  being the mean free path in the medium). It was realized a long time ago that this is analogous to the Landau-Pomeranchuk-Migdal (LPM) effect known from QED. In particular, the medium-induced coherent is suppressed by a factor  $1/\sqrt{\omega}$  as compared to the 1-scattering spectrum due to destructive interferences between the  $N_{\text{coh}}$  scattering centers. The BDMPS-Z spectrum [11, 12, 13, 14] mentioned above, which takes into account the non-Abelian LPM effect, has been the main ingredient in most studies of parton energy loss in the quark-gluon plasma.

For the study of jet evolution in heavy-ion collisions it therefore seems imperative to incorporate both the transverse and longitudinal coherence phenomena, as discussed above. However, such a unified approach is missing to date. Only recently, in [19, 20], were both coherences considered together in the context of antenna radiation in medium. Let us here merely point out a general analogy between the two phenomena. Note how the transverse and longitudinal wavelengths,  $\lambda_{\perp}$  and  $\lambda_{\parallel} \sim t_{\text{form}}$ , each are sensitive to the number of emitters and the number of scattering centers, respectively, determining the breakdown of independent radiation (in the former case) or scattering (in the latter) and the onset of coherence in both cases. In this work, we shall address the issue of both transverse and longitudinal coherences in the same setup, which we argue is the building block of in-medium jet physics.

### 3. Emission amplitude from classical Yang-Mills equations

As in our previous works [19, 20], we shall proceed in the framework of the classical Yang-Mills (CYM) equations, applicable for soft gluon radiation off an energetic charge [18]. First, let us recall the amplitude of emitting a gluon with momentum  $k \equiv (\omega, \vec{k})$ , given by the standard reduction formula,

$$\mathcal{M}_{\lambda}^a(\vec{k}) = \lim_{k^2 \rightarrow 0} \int d^4x e^{ik \cdot x} \square_x A_{\mu}^a(x) \epsilon_{\lambda}^{\mu}(\vec{k}), \quad (1)$$

where  $\epsilon_{\lambda}^{\mu}(\vec{k})$  is the gluon polarization vector while  $A_{\mu}^a$ , the classical gauge field, is the solution of the CYM equations,

$$[D_{\mu}, F^{\mu\nu}] = J^{\nu}, \quad (2)$$

with  $D_{\mu} \equiv \partial_{\mu} - igA_{\mu}$  and  $F_{\mu\nu} \equiv \partial_{\mu}A_{\nu} - \partial_{\nu}A_{\mu} - ig[A_{\mu}, A_{\nu}]$ . The covariantly conserved current, i.e.,  $[D_{\mu}, J^{\mu}] = 0$ , describes the projectiles.

We shall set our calculation in the light-cone gauge (LCG)  $A^+ = 0$ ,<sup>1</sup> where only the transverse polarization contribute to the cross-section, and  $\sum_{\lambda} \epsilon_{\lambda}^i(\epsilon_{\lambda}^j)^* = \delta^{ij}$ , where  $i(j) = 1, 2$ . Then the differential gluon radiation spectrum is given by

---

<sup>1</sup>The light-cone decomposition of the 4-vector  $x \equiv (x^0, x^1, x^2, x^3)$  is defined as  $x \equiv (x^+, x^-, \mathbf{x})$ , where  $x^{\pm} \equiv (x^0 \pm x^3)/\sqrt{2}$  and  $\mathbf{x} = (x^1, x^2)$ .

$$dN = \sum_{\lambda=1,2} |\mathcal{M}_\lambda^a(\vec{k})|^2 \frac{d^3k}{2(2\pi)^3 k^+}, \quad (3)$$

where the phase space is  $d^3k \equiv d^2\mathbf{k} dk^+$ .

Consider then an energetic  $q\bar{q}$  pair with momenta  $p \equiv (E, \vec{p})$  and  $\bar{p} \equiv (\bar{E}, \vec{\bar{p}})$ , respectively, created in the splitting of a highly virtual photon or gluon, generated in a hard process and moving in the  $+z$  direction. In the infinite energy limit, or equivalently for soft gluon radiation, this virtual state has a life-time too short to be resolved by the emitted gluon. Indeed, for soft gluons the pair looks like if it was produced instantaneously at  $t = 0$ . This property is the basis of soft-collinear factorization.

In the absence of the medium, the classical eikonalized current that describes the pair created at time  $t_0 = 0$  reads  $J_{(0)}^\mu = J_{q(0)}^\mu + J_{\bar{q}(0)}^\mu + J_{3(0)}^\mu$ , where, e.g., the quark vacuum current reads

$$J_{q(0)}^{\mu,a} = g \frac{p^\mu}{E} \delta^{(3)}(\vec{x} - \frac{\vec{p}}{E}t) \Theta(t) Q_q^a. \quad (4)$$

In momentum space the total current reads

$$J_{(0)}^{\mu,a}(k) = -ig \left( \frac{p^\mu}{p \cdot k + i\epsilon} Q_q^a + \frac{\bar{p}^\mu}{\bar{p} \cdot k + i\epsilon} Q_{\bar{q}}^a - \frac{p_3^\mu}{p_3 \cdot k + i\epsilon} Q_3^a \right), \quad (5)$$

where  $Q_q$  denotes the color charge vector of the quark (and, analogously,  $Q_{\bar{q}}$  for the antiquark). The third component of the current is needed for charge conservation, such that  $k \cdot J_{(0)} = 0$  which leads to  $Q_q + Q_{\bar{q}} = Q_3$ , while four-momentum conservation implies  $E_3 = E + \bar{E}$  and  $\vec{p}_3 = -\vec{p} - \vec{\bar{p}}$ . For a singlet antenna  $Q_3 = 0$ . In the case of a colored antenna, the third component of the current does not contribute in the frame where  $p_3 \approx (0, p_3^-, \mathbf{0})$  because of the gauge choice.

Taking the square of the total color charge vector, it is therefore possible to obtain the scalar product of two different charges, which in our case are

$$Q_q \cdot Q_{\bar{q}} = \begin{cases} -C_F & \text{singlet antenna } (\gamma^* \rightarrow q\bar{q}) \\ -C_F + C_A/2 & \text{octet antenna } (g^* \rightarrow q\bar{q}), \end{cases} \quad (6)$$

where  $C_F \equiv (N_c^2 - 1)/2N_c$  and  $C_A \equiv N_c$  are the fundamental and adjoint color charges of SU(3). The above reasoning can be extended to arbitrary color configurations of the particles involved.<sup>2</sup>

We shall focus on the the region of small angles defined by:  $p^+, \bar{p}^+ \gg |\mathbf{p}|, |\mathbf{\bar{p}}| \gg k^+ \gg |\mathbf{k}|$ . This is suitable in intrajet physics where one deals mainly with collimated particles. The  $q\bar{q}$  pair + gluon system is then strongly collimated

<sup>2</sup>E.g., the charge scalar product for a pure gluon antenna, i.e.,  $g^* \rightarrow g_1 g_2$ , is simply  $Q_{g_1} \cdot Q_{g_2} = -C_A/2$ , while gluon radiation off a quark,  $q^* \rightarrow qg$ , yields  $Q_q \cdot Q_g = -C_F/2$ .

in the  $+z$  direction [18]. A systematic way to perform this limit is to boost the medium in the opposite direction. Since we are only interested in asymptotic states, i.e., in probing the field  $A^a(x)$  at large times,  $x^+ \rightarrow \infty$ , the amplitude (A.1) can be rewritten in a more convenient form (cf. Appendix Appendix A)

$$\mathcal{M}_\lambda^a(\vec{k}) = \int_{x^+=+\infty} dx^- d^2\mathbf{x} e^{ik \cdot x} 2\partial_x^+ \mathbf{A}^a(x) \cdot \epsilon_\lambda(\vec{k}), \quad (7)$$

for on-shell gluons, i.e.,  $k^2 = 0$ . With the gauge choice above only the transverse component of the gauge field is dynamical. Its linear response to the medium interaction reads [18]

$$\square A^i - 2ig [A_{\text{med}}^-, \partial^+ A^i] = -\frac{\partial^i}{\partial^+} J^+ + J^i, \quad (8)$$

where the medium field  $A_{\text{med}}^\mu$  only has a negative light-cone component which, in the limit considered above, is related to the medium color source density through the Poisson equation  $-\partial^2 A_{\text{med}}^-(x^+, \mathbf{x}) = \rho_{\text{med}}(x^+, \mathbf{x})$  [18]. In Fourier space it reads

$$A_{\text{med}}^-(q) = 2\pi \delta(q^+) \int_0^\infty dx^+ \mathcal{A}_{\text{med}}(x^+, \mathbf{q}) e^{iq^- x^+}. \quad (9)$$

The current is found from the continuity relation,  $\partial_\mu J^\mu = ig[A_{\text{med}}^-, J^+]$ , which can be solved recursively [20] with

$$J_{q(m)}^\mu = ig \frac{p^\mu}{p \cdot \partial} [A_{\text{med}}^-, J_{q(m-1)}^+], \quad (10)$$

where the subscript  $m$  denotes the order of the expansion in the medium field. For  $m > 0$ , in momentum space we get

$$J_{q(m)}^{\mu,a}(k) = -(ig)^{m+1} \frac{p^\mu}{p \cdot k} \left[ \prod_{i=1}^m \int \frac{d^2\mathbf{q}_i}{(2\pi)^2} \int_0^{x_{i+1}^+} dx_i^+ \right. \\ \left. \times e^{i\frac{p \cdot \mathbf{q}_i}{p^+} x_i^+} T \cdot \mathcal{A}_{\text{med}}(x_i^+, \mathbf{q}_i) \right]^{ab} Q_q^b e^{i\frac{p \cdot k}{p^+} x_m^+}, \quad (11)$$

where  $x_{m+1}^+ = L$  is the total medium length and  $T$  are the generators of  $SU(3)$  in the adjoint representation. Summing over the number of possible interactions,  $J_q^{\mu,a} = \sum_{m=0}^\infty J_{q(m)}^{\mu,a}$ , yields

$$J_q^{\mu,a}(k) = -ig \frac{p^\mu}{p \cdot k} \left[ \delta^{ab} + \int_0^L dx^+ e^{i\frac{p \cdot k}{p^+} x^+} \partial^- U_p^{ab}(x^+, 0) \right] Q_q^b, \quad (12)$$

where  $U_p$  denotes the Wilson line, in the adjoint representation, tracing the trajectory of the quark which is given by its momentum  $p$ . It is found from the general definition of the Wilson line in the adjoint representation, given by

$$U(x^+, 0; [\mathbf{r}]) \equiv \mathcal{P}_\xi \exp \left[ ig \int_0^{x^+} d\xi T \cdot A_{\text{med}}^-(\xi, \mathbf{r}(\xi)) \right], \quad (13)$$

where  $[\mathbf{r}]$  defines the trajectory of the probe, by setting

$$U_p(x^+, 0) \equiv U(x^+, 0; [\mathbf{r}]) \Big|_{\mathbf{r}(\xi)=\xi \mathbf{p}/p^+}. \quad (14)$$

Note that color indices are omitted when they are obvious to alleviate the notations. The general medium-modified current, given in Eq. (12), was obtained for the first time in [20]. In coordinate space, (12) simplifies to

$$J_q^\mu(x) = U_p(x^+, 0) J_{q(0)}^\mu(x), \quad (15)$$

with the vacuum current defined in Eq. (4). Note that  $U_p(x^+, 0) = U_p(L, 0)$  for  $x^+ > L$ . Returning presently to the calculation of the gauge field, the solution of Eq. (8) takes the following form

$$A_q^i(x) = \int d^4y G(x, y) \tilde{J}_q^i(y), \quad (16)$$

with the modified current reads

$$\tilde{J}^i = -\frac{\partial^i}{\partial^+} J^+ + J^i, \quad (17)$$

and the retarded Green's function is defined by

$$(\square - 2igT \cdot A_{\text{med}}^- \partial^+) G(x, y) = \delta^{(4)}(x - y). \quad (18)$$

Note that this Green's function is invariant under translations along the  $x^-$  direction due to the fact that the medium field depends only on  $x^+$  and  $\mathbf{x}$ . This translational symmetry yields the conservation of the gluon energy  $k^+$  while traversing the medium and holds as long as  $k^+ \gg |\mathbf{k}|$ . This property allows us to introduce another useful Green's function

$$\mathcal{G}(x^+, \mathbf{x}; y^+, \mathbf{y}|k^+) = \int_{-\infty}^{+\infty} dx^- e^{i(x-y)^- k^+} 2\partial_x^+ G(x, y), \quad (19)$$

which obeys the following Schrödinger-like equation

$$\left( i\partial^- + \frac{\partial^2}{2k^+} + gT \cdot A_{\text{med}}^- \right) \mathcal{G}(x^+, \mathbf{x}; y^+, \mathbf{y}|k^+) = i\delta(x^+ - y^+) \delta(\mathbf{x} - \mathbf{y}). \quad (20)$$

The solution to (20) is well known and can be expressed in terms of a path integral in the transverse plane, leading to

$$\mathcal{G}(x^+, \mathbf{x}; y^+, \mathbf{y}|k^+) = \int \mathcal{D}[\mathbf{r}] \exp \left[ i \frac{k^+}{2} \int_{y^+}^{x^+} d\xi \dot{\mathbf{r}}^2(\xi) \right] U(x^+, y^+; [\mathbf{r}]), \quad (21)$$

where  $U(x^+, y^+; [\mathbf{r}])$  is defined in Eq. (13) and the boundary conditions are  $\mathbf{r}(y^+) = \mathbf{y}$  and  $\mathbf{r}(x^+) = \mathbf{x}$ . The Green's function  $\mathcal{G}$  describes simultaneously the color rotation of the emitted gluon together with its Brownian motion in the transverse plane due to the interactions with the background field [15, 16, 18].

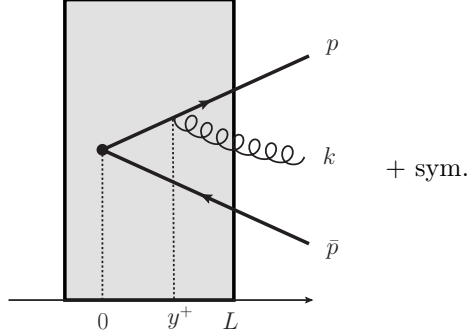


Figure 1: The gluon radiation amplitude off an energetic  $q\bar{q}$  pair created at  $t = 0$  in a medium of length  $L$ . The gluon is emitted at time  $y^+$  (cf. Eq. (23)).

Inserting the field solution (16) into Eq. (7), we obtain the amplitude

$$\begin{aligned} \mathcal{M}_{\lambda,q}^a(\vec{k}) &= \int_{x^+=+\infty} d^2\mathbf{x} e^{ik^-x^+ - i\mathbf{k}\cdot\mathbf{x}} \int dy^+ dy^- d^2\mathbf{y} e^{ik^+y^-} \\ &\times \mathcal{G}^{ab}(x^+, \mathbf{x}; y^+, \mathbf{y} | k^+) U_p^{bc}(y^+, 0) \epsilon_\lambda \cdot \tilde{\mathbf{J}}_{q(0)}^c(\mathbf{y}), \end{aligned} \quad (22)$$

where  $k^- = \mathbf{k}^2/2k^+$  for the on-shell gluon. Simplifying further by integrating over  $y^-$  and  $\mathbf{y}$  making use of the vacuum current given in Eq. (4), the amplitude in Eq. (22) finally becomes

$$\begin{aligned} \mathcal{M}_{\lambda,q}^a(\vec{k}) &= \frac{g}{k^+} \int_{x^+=+\infty} d^2\mathbf{x} e^{ik^-x^+ - i\mathbf{k}\cdot\mathbf{x}} \int_0^{+\infty} dy^+ e^{i\frac{k^+p^-}{p^+}y^+} \\ &\times \epsilon_\lambda \cdot (i\partial_{\mathbf{y}} + k^+\mathbf{n}) \mathcal{G}^{ab}(x^+, \mathbf{x}; y^+, \mathbf{y} | k^+) \Big|_{\mathbf{y}=\mathbf{n}y^+} U_p^{bc}(y^+, 0) Q_q^c, \end{aligned} \quad (23)$$

where we have introduced the dimensionless vector  $\mathbf{n} = \mathbf{p}/p^+$  (equivalently  $\bar{\mathbf{n}} = \bar{\mathbf{p}}/\bar{p}^+$  for the antiquark). The corresponding amplitude for the antiquark,  $\mathcal{M}_{\lambda,\bar{q}}^a(\vec{k})$ , is found by substituting  $p$  with  $\bar{p}$  and  $Q_q$  with  $Q_{\bar{q}}$ .

Summarizing, the amplitude in Eq. (23) describes the propagation of the quark, with color charge  $Q_q$ , from the beginning of the medium up to a point  $y^+$  where the gluon emission takes place, and the further propagation of the gluon through the medium out to the detector. The process is depicted in Fig. 1. Note that  $y^+ > L$  implies gluon vacuum emission off an in-medium color rotated quark current.

#### 4. The antenna spectrum in the presence of a medium

In the following, we assume a simple model for the medium namely that it is made out of uncorrelated, static scattering centers (in the spirit of the Glauber

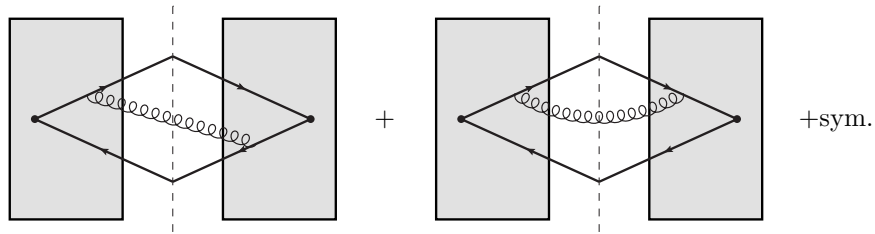


Figure 2: Representation of the various contributions to the in-medium antenna spectrum. The first diagram stands for the interference part  $\mathcal{J}$ , while the second one stands for the BDMPs part  $\mathcal{R}_q$ . The rest symbolizes the symmetric configuration.

picture). Then, we can treat the background field,  $\mathcal{A}_{\text{med}}$ , as a Gaussian white noise. The medium average of two fields can therefore be written as

$$\langle \mathcal{A}_{\text{med}}^a(x^+, \mathbf{q}) \mathcal{A}_{\text{med}}^{*b}(x'^+, \mathbf{q}') \rangle \equiv \delta^{ab} n(x^+) \delta(x^+ - x'^+) (2\pi)^2 \delta^{(2)}(\mathbf{q} - \mathbf{q}') \mathcal{V}^2(\mathbf{q}), \quad (24)$$

where  $\mathcal{V}(\mathbf{q})$  is the medium interaction potential and  $n(x^+)$  is the 3-dimensional density of scattering centers. Usually,  $\mathcal{V}(\mathbf{q})$  is chosen to be a Debye-screened Coulomb potential [15, 16, 17].

Considering for the moment the most general case of a virtual gluon splitting into a quark-antiquark pair,  $g^* \rightarrow q\bar{q}$ , the spectrum can be written in the standard form [21] as

$$dN = \frac{\alpha_s}{(2\pi)^2} [C_F \mathcal{R}_{\text{sing}} + C_A \mathcal{J}] \frac{d^3 k}{(k^+)^3}, \quad (25)$$

where we have introduced the spectrum of a color-singlet antenna

$$\mathcal{R}_{\text{sing}} = \mathcal{R}_q + \mathcal{R}_{\bar{q}} - 2\mathcal{J}, \quad (26)$$

and  $C_F \mathcal{R}_q = (k^+)^2 \langle |\mathcal{M}_q|^2 \rangle$ ,  $C_F \mathcal{R}_{\bar{q}} = (k^+)^2 \langle |\mathcal{M}_{\bar{q}}|^2 \rangle$  and  $(-C_F + C_A/2) \mathcal{J} = (k^+)^2 \langle \text{Re} \mathcal{M}_q^* \mathcal{M}_{\bar{q}} \rangle$  represent independent radiation off the quark, the antiquark and the interferences, respectively. Here,  $\langle \dots \rangle$  signify medium averages as defined in Eq. (24). Note that the first term in Eq. (25) is proportional to the color charge of the quark/antiquark constituents whereas the second term is proportional to the total charge of the antenna. The total spectrum (25), with its various components, is depicted in Fig. 2.

Because of the symmetries between the quark and the antiquark emission amplitudes we only need to evaluate the cross term,  $\mathcal{J}$ , represented in the left

panel of Fig. 2. Using Eq. (23) we obtain

$$\begin{aligned}
\mathcal{J} = \text{Re} & \left\{ \int_0^{+\infty} dy'^+ \int_0^{y'^+} dy^+ \int d^2\mathbf{x} \int d^2\mathbf{x}' e^{-i\mathbf{k}\cdot(\mathbf{x}-\mathbf{x}') + ik^+(\mathbf{n}^2 y^+ - \bar{\mathbf{n}}^2 y'^+)/2} \right. \\
& \times (i\boldsymbol{\partial}_y + k^+ \mathbf{n}) \cdot (-i\boldsymbol{\partial}_{y'} + k^+ \bar{\mathbf{n}}) \frac{1}{N_c^2 - 1} \langle \text{Tr} \mathcal{G}(\infty, \mathbf{x}; y^+, \mathbf{y}|k^+) U_p(y^+, 0) \\
& \left. \times U_{\bar{p}}^\dagger(y'^+, 0) \mathcal{G}^\dagger(\infty, \mathbf{x}'; y'^+, \mathbf{y}'|k^+) \rangle \right\} + \text{sym.}, \quad (27)
\end{aligned}$$

where the gluon is emitted at  $y^+$  in the amplitude and at  $y'^+ > y^+$  in the complex conjugate. The symmetric part, i.e., interchanging  $q \leftrightarrow \bar{q}$  in all relevant quantities, accounts for the opposite  $y^+$  ordering. Then the medium average can be split into three pieces, namely

$$\begin{aligned}
\frac{1}{N_c^2 - 1} \langle \text{Tr} \mathcal{G}(\infty, \mathbf{x}; y^+, \mathbf{y}|k^+) U_p(y^+, 0) U_{\bar{p}}^\dagger(y'^+, 0) \mathcal{G}^\dagger(\infty, \mathbf{x}'; y'^+, \mathbf{y}'|k^+) \rangle = \\
\int d^2\mathbf{z} \frac{1}{N_c^2 - 1} \langle \text{Tr} \mathcal{G}(\infty, \mathbf{x}; y^+, \mathbf{z}|k^+) \mathcal{G}^\dagger(\infty, \mathbf{x}'; y'^+, \mathbf{y}'|k^+) \rangle \\
\times \frac{1}{N_c^2 - 1} \langle \text{Tr} \mathcal{G}(y'^+, \mathbf{z}; y^+, \mathbf{y}|k^+) U_{\bar{p}}^\dagger(y'^+, y^+) \rangle \\
\times \frac{1}{N_c^2 - 1} \langle \text{Tr} U_p(y^+, 0) U_{\bar{p}}^\dagger(y^+, 0) \rangle, \quad (28)
\end{aligned}$$

where we have used the following identity

$$\mathcal{G}(\infty, \mathbf{x}; 0, \mathbf{y}|k^+) = \int d^2\mathbf{z} \mathcal{G}(\infty, \mathbf{x}; z^+, \mathbf{z}|k^+) \mathcal{G}(z^+, \mathbf{z}; 0, \mathbf{y}|k^+). \quad (29)$$

In the region from 0 to  $y^+ < y'^+$ , the gluon is not produced yet, neither in the amplitude nor in the complex conjugate. The pure quark-antiquark interference is described by

$$\frac{1}{N_c^2 - 1} \langle \text{Tr} U_p(y^+, 0) U_{\bar{p}}^\dagger(y^+, 0) \rangle = 1 - \Delta_{\text{med}}(y^+, 0), \quad (30)$$

where  $\Delta_{\text{med}}$  was defined in [20] as the decoherence rate of the antenna,

$$\Delta_{\text{med}}(y^+, 0) \equiv 1 - \exp \left[ -\frac{1}{2} \int_0^{y^+} d\xi n(\xi) \sigma(\delta\mathbf{n} \xi) \right], \quad (31)$$

with  $\delta\mathbf{n} = \mathbf{n} - \bar{\mathbf{n}}$ . The modulus of this vector corresponds roughly to the opening angle of the pair, i.e.,  $|\delta\mathbf{n}| \equiv \sin \theta_{q\bar{q}} \sim \theta_{q\bar{q}}$ . We will discuss the physical meaning of this coefficient below and in Section 5. The decoherence rate depends on the dipole cross-section  $\sigma$ , which is given by

$$\sigma(\delta\mathbf{n} \xi) = 2\alpha_s C_A \int \frac{d^2\mathbf{q}}{(2\pi)^2} \mathcal{V}^2(\mathbf{q}) [1 - \cos(\delta\mathbf{n} \cdot \mathbf{q} \xi)]. \quad (32)$$

For consistency with previous calculations, we note that  $n(\xi) \sigma(\mathbf{r}) \approx \frac{1}{2} \hat{q}(\xi) \mathbf{r}^2$  in the multiple soft scattering approximation [26], where  $\hat{q}$  is the medium transport parameter probing the accumulated transverse momentum squared per unit length.

From  $y^+$  to  $y'^+$ , there is an interference between gluon and antiquark-medium interactions, which is described by

$$\begin{aligned} \frac{1}{N_c^2 - 1} \langle \text{Tr} \mathcal{G}(y'^+, \mathbf{z}; y^+, \mathbf{y} | k^+) U_{\bar{p}}^\dagger(y'^+, y^+) \rangle = \\ \exp \left\{ i k^+ \bar{\mathbf{n}} \cdot [\bar{\mathbf{z}}(y'^+) - \bar{\mathbf{y}}(y^+)] + i \frac{k^+}{2} \bar{\mathbf{n}}^2 (y'^+ - y^+) \right\} \\ \times \mathcal{K}(y'^+, \bar{\mathbf{z}}(y'^+); y^+, \bar{\mathbf{y}}(y^+) | k^+) , \end{aligned} \quad (33)$$

where  $\bar{\mathbf{z}}(y'^+) = \mathbf{z} - \bar{\mathbf{n}} y'^+$  and  $\bar{\mathbf{y}}(y^+) = \mathbf{y} - \bar{\mathbf{n}} y^+$ . The gluon multiple scattering with the medium is taken into account by the path integral  $\mathcal{K}$  [15, 16, 17], given by

$$\mathcal{K}(y'^+, \mathbf{z}; y^+, \mathbf{y} | k^+) = \int \mathcal{D}[\mathbf{r}] \exp \left[ \int_{y^+}^{y'^+} d\xi \left( i \frac{k^+}{2} \dot{\mathbf{r}}^2(\xi) - \frac{1}{2} n(\xi) \sigma(\mathbf{r}) \right) \right] , \quad (34)$$

which describes the Brownian motion of the gluon the transverse plane from  $\mathbf{r}(y^+) = \mathbf{y}$  to  $\mathbf{r}(y'^+) = \mathbf{z}$ . Finally, the medium average involving the gluon line element from  $y'^+$  to  $+\infty$  reads

$$\begin{aligned} \int d^2 \mathbf{x} \int d^2 \mathbf{x}' \frac{e^{-i \mathbf{k} \cdot (\mathbf{x} - \mathbf{x}')}}{N_c^2 - 1} \langle \text{Tr} \mathcal{G}(+\infty, \mathbf{x}; y'^+, \mathbf{z} | k^+) \mathcal{G}^\dagger(+\infty, \mathbf{x}'; y'^+, \mathbf{y}' | k^+) \rangle = \\ \exp \left[ -i \mathbf{k} \cdot (\mathbf{z} - \mathbf{y}') - \frac{1}{2} \int_{y'^+}^{+\infty} d\xi n(\xi) \sigma(\mathbf{z} - \mathbf{y}') \right] . \end{aligned} \quad (35)$$

For more details on medium averages see, for instance, [15, 18].

Putting everything together and after some straightforward algebra we get

$$\begin{aligned} \mathcal{J} = \text{Re} \left\{ \int_0^\infty dy'^+ \int_0^{y'^+} dy^+ (1 - \Delta_{\text{med}}(y^+, 0)) \right. \\ \times \int d^2 \mathbf{z} \exp \left[ -i \bar{\boldsymbol{\kappa}} \cdot \mathbf{z} - \frac{1}{2} \int_{y'^+}^\infty d\xi n(\xi) \sigma(\mathbf{z}) + i \frac{k^+}{2} \delta \mathbf{n}^2 y^+ \right] \\ \left. \times (\partial_{\mathbf{y}} - i k^+ \delta \mathbf{n}) \cdot \partial_{\mathbf{z}} \mathcal{K}(y'^+, \mathbf{z}; y^+, \mathbf{y} | k^+) \Big|_{\mathbf{y} = \delta \mathbf{n} y^+} \right\} + \text{sym.} , \end{aligned} \quad (36)$$

where  $\bar{\boldsymbol{\kappa}} = \mathbf{k} - \bar{x} \bar{\mathbf{p}}$  (similarly,  $\boldsymbol{\kappa} = \mathbf{k} - x \mathbf{p}$ ), and we have defined the light-cone momentum fractions  $x = k^+ / p^+$  and  $\bar{x} = k^+ / \bar{p}^+$ . Equation (36) is the main result of this paper. It describes the interference pattern between in-medium gluon radiation off a quark and an antiquark constituting a collimated antenna.

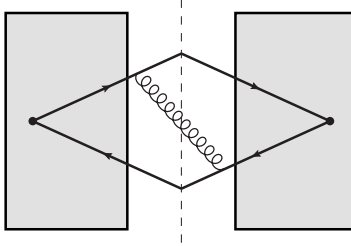


Figure 3: Non-vanishing contribution to the medium-induced gluon spectrum in the opaque limit as well as the soft limit. Only gluons whose formation time  $t_{\text{form}} \gtrsim L$ , contribute in both cases.

Following a similar procedure as described above for  $\mathcal{R}_q$ , we easily get the spectrum off a single quark, given by

$$\mathcal{R}_q = 2 \operatorname{Re} \left\{ \int_0^\infty dy'^+ \int_0^{y'^+} dy^+ \int d^2z \exp \left[ -i\boldsymbol{\kappa} \cdot \mathbf{z} - \frac{1}{2} \int_{y^+}^\infty d\xi n(\xi) \sigma(\mathbf{z}) \right] \right. \\ \left. \times \boldsymbol{\partial}_y \cdot \boldsymbol{\partial}_z \mathcal{K}(y'^+, \mathbf{z}; y^+, \mathbf{y} = \mathbf{0} | k^+) \right\}, \quad (37)$$

where the factor 2 accounts for the opposite  $y^+$  ordering. The antiquark spectrum  $\mathcal{R}_{\bar{q}}$  is found analogously. This corresponds to the BDMPS-Z spectrum, in accordance with [15, 16, 17].

The various parts of the spectrum (25), given in Eq. (36) and Eq. (37), have many features in common. As mentioned before, both account for multiple scattering of all partons involved in the process—most importantly, the gluon—and therefore properly account for longitudinal coherence, which is reflected in the LPM suppression phenomenon.

Remarkably, apart from the color charge the interference terms of the antenna spectrum (36) differs from the BDMPS-Z spectrum (37) mainly by two suppression factors that encompass the main elements of transverse coherence in medium. Firstly, the factor  $1 - \Delta_{\text{med}}(y^+, 0)$  is sensitive to the medium density and vanishes in the opaque limit causing all interferences to disappear (for details, see Section 5). Secondly, the phase  $\exp(ik^+ \delta \mathbf{n}^2 y^+ / 2)$  defines a new scale

$$\omega_{\text{coh}} \sim (\theta_{q\bar{q}}^2 L)^{-1}, \quad (38)$$

above which medium-induced interferences are suppressed exponentially.

The role played by the interferences,  $\mathcal{J}$ , as compared to the independent spectra,  $\mathcal{R}_q$  and  $\mathcal{R}_{\bar{q}}$ , is most prominent in the soft limit,  $\omega \rightarrow 0$ . This was previously discussed in detail in [19, 20], where it was shown that the leading contribution to the spectrum is given by the diagram in Fig. 3 where the gluon emission takes place outside the medium (cf. Appendix Appendix B). In this case, the independent spectra,  $\mathcal{R}_q$  and  $\mathcal{R}_{\bar{q}}$ , simply reduce to the corresponding

vacuum quantities,  $\mathcal{R}_q^{\text{vac}}$  and  $\mathcal{R}_{\bar{q}}^{\text{vac}}$ , given by (41). In effect, the medium-induced part vanishes. This is a manifestation of the LPM interference. The functional form of the interference terms, on the other hand, also become vacuumlike yet the influence of the medium remains as an overall multiplicative factor  $1 - \Delta_{\text{med}}$ , controlling the onset of transverse decoherence. Since  $\Delta_{\text{med}}$  is bound by unitarity, interferences for soft gluon emissions vanish with increasing  $\Delta_{\text{med}}$ , or medium density, resulting in an incoherent sum of independent radiative spectra off the quark and the antiquark. This justifies the interpretation of this quantity as a decoherence rate [20].

Finally, note that in the limit of vanishing opening angle,  $|\delta n| \sim \theta_{q\bar{q}} \rightarrow 0$ , the color singlet spectrum vanishes, while in the octet case what remains is the BDMPS-Z spectrum off the total charge of the pair, namely  $C_A(\mathcal{R}_q + \mathcal{R}_{\bar{q}})/2$ .

## 5. The limit of infinitely opaque medium

It is worthwhile exploring the limit where the density of the scattering centers tends to infinity for a finite medium length in more detail. This situation corresponds to a vanishing mean free path. In the BDMPS-Z scenario the medium-induced gluon radiation is suppressed for gluon formation times larger than the medium length  $L$ . Hence, only gluons that undergo multiple scatterings in the medium are freed. The rescattering of the gluon is therefore a key feature yielding a broader gluon emission angle for denser media [11, 12, 26]. This implies that the BDMPS-Z spectrum is strongly suppressed in opaque media.

Indeed, when  $n(\xi) \rightarrow \infty$  for  $\xi < L$  the Green's function  $\mathcal{K}$  drops exponentially. We are therefore left only with the region  $y^+ > L$  in which  $n(\xi) = 0$ , yielding

$$\begin{aligned} \mathcal{R}_q \approx 2 \text{Re} \left\{ \int_L^\infty dy'^+ \int_L^{y'^+} dy^+ \int d^2 \mathbf{u} e^{-i\boldsymbol{\kappa} \cdot \mathbf{u}} \right. \\ \left. \times \boldsymbol{\partial}_y \cdot \boldsymbol{\partial}_u \mathcal{K}_0(y'^+, \mathbf{u}; y^+, \mathbf{y}|k^+) \Big|_{\mathbf{y}=0} \right\}, \end{aligned} \quad (39)$$

where

$$\mathcal{K}_0(y'^+, \mathbf{u}; y^+, \mathbf{y}|k^+) = \frac{k^+}{2\pi i(y' - y)^+} \exp \left[ i \frac{k^+ (\mathbf{u} - \mathbf{y})^2}{2(y' - y)^+} \right]. \quad (40)$$

Since  $\mathcal{K}_0$  is invariant under translation we get

$$\begin{aligned} \mathcal{R}_q &= \boldsymbol{\kappa}^2 2 \text{Re} \int_L^\infty dy'^+ \int_L^{y'^+} dy^+ e^{-i \frac{\boldsymbol{\kappa}^2}{2k^+} (y' - y)^+} \\ &= 2 \frac{p^+ k^+}{p \cdot k}, \end{aligned} \quad (41)$$

where we have used that  $\boldsymbol{\kappa}^2 = 2x(p \cdot k)$  in the last line. This is nothing but the radiation spectrum off a quark in vacuum  $\mathcal{R}_q^{\text{vac}}$  [21]. In other words, the medium-induced part vanishes in the opaque limit.

Let us turn now to the interferences. Following the same line of arguments we get

$$\begin{aligned} \mathcal{J} \approx & \text{Re} \left\{ \int_L^\infty dy'^+ \int_L^{y'^+} dy^+ (1 - \Delta_{\text{med}}(L, 0)) \right. \\ & \times \int d^2 \mathbf{u} \exp \left[ -i \bar{\mathbf{k}} \cdot \mathbf{u} + i \frac{k^+}{2} \delta \mathbf{n}^2 y^+ \right] \\ & \left. \times (\partial_{\mathbf{y}} - ik^+ \delta \mathbf{n}) \cdot \partial_{\mathbf{u}} \mathcal{K}_0(y'^+ - y^+, \mathbf{u} - \mathbf{y} | k^+) \Big|_{\mathbf{y}=\delta \mathbf{n} y^+} \right\} + \text{sym}. \quad (42) \end{aligned}$$

While the path integral tends to the same limit as in (39), the key observation is noting the importance of the medium decoherence parameter,  $\Delta_{\text{med}}$ , which goes to unity in the opaque limit  $\Delta_{\text{med}}(L, 0) \rightarrow 1$ , see (31). Overall, this leads to the disappearance of the interference terms,

$$\lim_{n(\xi) \rightarrow \infty} \mathcal{J} = 0, \quad (43)$$

i.e., the medium induced interferences cancel exactly the vacuum ones. Thus, the spectrum in the opaque limit simply reads

$$dN|_{\text{opaque}} = \frac{\alpha_s}{(2\pi)^2} C_F (\mathcal{R}_q^{\text{vac}} + \mathcal{R}_{\bar{q}}^{\text{vac}}) \frac{d^3 k}{(k^+)^3}, \quad (44)$$

i.e., it consists only of incoherent radiation off the antenna arms *as if* they were propagating independently in vacuum [20].

The simplicity of the result in Eq. (44) is striking and can be understood as a sort of memory loss effect [20]. Not only does the quark (“son”) lose sensitivity of the color charge of the antiquark (its “sibling”) but it also “forgets” about the color charge of the total charge of the pair, that of the “parent” gluon (note that the spectrum (44) is independent of the total color charge of the antenna). Remarkably, all medium effects cancel out leading to vacuumlike emissions. This result relies crucially on the inclusion of medium-induced radiative interferences. While (44) was previously only derived in the soft limit [20], here we have generalized this result to all gluon energies.

## 6. In-medium coherence: general discussion

Although the spectra (36) and (37) at first sight have a quite complicated structure, further insight can be gained by studying the relevant scales involved in the problem. It will be shown, that these scales can be related to coherence phenomena in both the longitudinal direction and the transverse plane and that they indicate how medium properties affect the shape of the spectrum in various regimes. As discussed previously in Section 2, transverse radiative coherence, in particular, plays a key role in jet physics in vacuum.

Let us for the moment consider the medium interactions of the gluon, common to both  $\mathcal{J}$  and  $\mathcal{R}_q$ , which we will discuss in the approximation of multiple soft scattering for convenience. The coherent interaction of the gluon with multiple scattering centers ordered in the longitudinal direction leads to the emergence of a characteristic gluon energy [11, 12, 26], namely

$$\omega_c \sim \hat{q}L^2. \quad (45)$$

Consequently, the BMDPS-Z spectrum is dominated by  $\omega < \omega_c$  and strongly suppressed above [15, 16, 17]. The emergence of  $\omega_c$  has a simple physical explanation in terms of the gluon formation time,  $t_{\text{form}}$ . For a BMDPS-Z gluon, formed mainly inside the medium, we have  $t_{\text{form}} \sim \sqrt{\omega/\hat{q}} < L$ , which implies that  $\omega < \omega_c$ .

The novel aspect of  $\mathcal{J}$ , which is missing in  $\mathcal{R}_q$ , has already briefly been touched upon in Section 4. While  $\mathcal{R}_q \rightarrow \mathcal{R}_q^{\text{vac}}$  when  $\omega \rightarrow 0$ , the existence of a soft divergence in  $\mathcal{J}$  implies medium-induced gluons with very long formation times,  $t_{\text{form}} \sim 1/\omega\theta^2 \gg L$ , where  $\theta$  is the gluon emission angle. Recalling that the medium-induced spectrum is suppressed inside the pair and falls off as  $1/\theta$  for  $\theta > \theta_{q\bar{q}}$  [19], the characteristic emission angle scales like  $\theta_{q\bar{q}}$ . Therefore,  $t_{\text{form}} > L$  corresponds to gluon energies smaller than

$$\omega_{\text{coh}} \sim (\theta_{q\bar{q}}^2 L)^{-1}, \quad (46)$$

which controls the onset of radiative coherence effects in the medium. This scale, as was already pointed out in Section 4, appears explicitly in the phase  $\exp(ik^+ \delta \mathbf{n}^2 y^+ / 2)$  in (36). There is, thus, a strong separation in formation times of typical BMDPS-Z gluons and soft ones. Given a typical configuration of a dense plasma, we assume that  $\omega_c \gg \omega_{\text{coh}}$ .

Seemingly, this leaves limited room for coherence effects of the antenna in the presence of a medium. As we shall demonstrate below, however, there is an important intermediate scale which extends significantly the region where coherence effects are at play. It is related to the observation that large-angle emissions are always sensitive to the total color charge of the antenna and, in effect, are coherent. In other words, these emissions are always subject to destructive interferences from emitters close in space. An example of the extended coherence regime is given in [19]: Namely, the total spectrum preserves its simple, vacuumlike shape, derived explicitly in the soft limit, up to sizable  $\omega$  due to a complex interplay between the various components of the spectrum.

Here, we argue that these cancellations take place as long as the typical BMDPS-Z emission angle  $\Theta_c \sim \sqrt{\hat{q}/\omega^3} > \theta_{q\bar{q}}$ . In this case, the BMDPS-Z gluons know about the existence of the other antenna emitter and are vulnerable to interference effects. It is only in the strictly opposite case, when  $\Theta_c < \theta_{q\bar{q}}$ , that the emitter radiates truly independently. This transition gives rise to a new scale, which is given by

$$\omega^* \sim \left( \frac{\hat{q}}{\theta_{q\bar{q}}^4} \right)^{1/3}. \quad (47)$$

We note the, somewhat surprising, relation between the various scales revealing the intricate interplay between the different phenomena at work

$$\omega^* = (\omega_{\text{coh}}^2 \omega_c)^{1/3}. \quad (48)$$

Furthermore, there exists a fixed point when  $\hat{q}_{\text{res}} = (\theta_{q\bar{q}}^2 L^3)^{-1}$  such that  $\omega_{\text{coh}} = \omega^* = \omega_c$ . This reflects a resonance between the maximum transverse momentum accumulated by the gluon in the plasma  $\sqrt{\hat{q}L}$  and the typical inverse transverse separation of the pair  $(\theta_{q\bar{q}}L)^{-1}$ .

Based on the discussion above, we are therefore able to identify the following hierarchy of scales, true as long as  $\hat{q} > \hat{q}_{\text{res}}$ <sup>3</sup>

$$\omega_{\text{coh}} < \omega^* < \omega_c, \quad (49)$$

which we interpret as follows (cf. Fig. (4)),

- The coherence regime,  $\omega < \omega_{\text{coh}}$ , where the spectrum is dominated by gluons formed at  $t_f > L$  in  $\mathcal{J}$  and it exhibits a geometrical separation of vacuum ( $\theta < \theta_{q\bar{q}}$ ) and coherent medium-induced radiation, which occurs at large angles ( $\theta > \theta_{q\bar{q}}$ ), leading to gradual decoherence of the pair radiation pattern [20]. Note that this decoherence phenomenon takes place in a region where color coherence is at work, in contrast with independent radiation at angles smaller than the pair opening angle (see the last point below).
- The regime of extended coherence,  $\omega_{\text{coh}} < \omega < \omega^*$ , displays the interplay between various components of the spectrum enforcing the vacuumlike angular distribution of the previous regime and an exponential drop of the medium-induced spectrum sets in. In this regime gluons are formed inside the medium within the time interval  $t^* < t_{\text{form}} < L$ , where  $t^* = (\hat{q} \theta_{q\bar{q}}^2)^{-1/3}$ . BDMPS-Z gluons are mainly radiated outside the pair and thus are suppressed due to transverse coherence.
- The incoherent BDMPS-Z regime,  $\omega^* < \omega$ : in this case the antenna spectrum is a incoherent superposition of BDMPS-Z spectrum off the quark and the antiquark augmented by the coherent vacuum spectrum  $\mathcal{R}_{\text{sing}}^{\text{vac}}$ . This occurs when the gluons that undergo multiple scattering in the medium are emitted at smaller angles than the opening angle of the pair such that they resolve the fine color structure of the pair. Here, medium-induced radiation takes place early, at  $t_{\text{form}} < t^*$ . We note that angular ordering property is not altered in this regime since large angle emissions are strongly suppressed (in contrast with the coherence regime).

The above identifications give rise to a rich range of possibilities. As an exercise, let us therefore quickly motivate the results of the previous section in

---

<sup>3</sup>Note that  $\omega_c < \omega^* < \omega_{\text{coh}}$  is also possible. In this special case, the BDMPS-Z spectrum is always strongly suppressed.

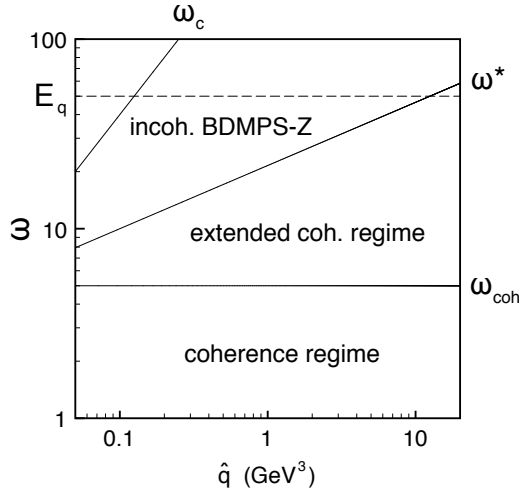


Figure 4: Diagram representing the various regimes of the antenna radiation spectrum as a function of the gluon energy  $\omega$  and the transport coefficient  $\hat{q}$  (medium density). The scales  $\omega_c$ ,  $\omega^*$  and  $\omega_{\text{coh}}$  are given in Eqs. (45), (47) and (46), respectively. The dashed line represents a possible quark (antiquark) energy,  $E_q = 50$  GeV, that sets the upper bound for gluon energies. We have considered a pair opening angle  $\theta_{q\bar{q}} = 0.1$  and a medium length  $L = 4$  fm.

light of these considerations. When we let  $\hat{q} \rightarrow \infty$ , as in Section 5, consequently  $\omega^* \rightarrow \infty$ . Thus, the incoherent BDMPS-Z regime vanishes and we are only left with the decoherent vacuumlike spectrum which, in this limit, is the superposition of independent spectra off the quark and antiquark *as if* in vacuum, in correspondence with (44). The general situation is depicted in Fig. 4. Clearly, the regime of extended coherence grows with  $\hat{q}$ , opening up the phase space for coherent gluon emissions and thus, vacuumlike gradual decoherence.

## 7. Conclusions

To summarize, we have computed the emission spectrum off a  $q\bar{q}$  antenna in both color singlet and octet representations traversing an arbitrary dense and colored medium. This generalizes our previous results in [19], which were valid only for dilute media, and in [20], where we only considered the strictly soft limit.

Our main result is the interference spectrum, given in Eq. (36), which encompasses two distinct types of QCD coherence. On one hand, the transverse momentum broadening of the gluon described by the path integral  $\mathcal{K}$  is a manifestation of the longitudinal coherence leading to LPM suppression.

On the other hand, due to the proper treatment of the transverse dynamics of the pair,  $\mathcal{J}$  additionally contains interference between emissions off two different projectiles. The latter, radiative interferences are crucial for building up the vacuum cascade accounting in a proper way for QCD coherence. Our results

thus establish generically how these effects are modified in the presence of an arbitrarily dense and deconfined medium.

Thanks to an analysis of the relevant scales involved in the problem, the following physical picture emerges. Considering for the moment only the singlet part of the spectrum (25), we observed that transverse coherence effects are always present at large angles since in this region one is always sensitive to the color charge of several emitters. This leads to an extended regime of coherent medium-induced emissions, for  $\omega \lesssim \omega^*$ , where the spectrum remains vacuumlike at large angles (also, see [19]). Taken together with the vacuum emissions, which obey angular ordering, this results in a gradual onset of decoherence of the antenna radiation with increasing medium density [20].

In the opposite case of small angle emissions, i.e., with  $\omega^* < \omega$ , the medium-induced spectrum becomes the incoherent superposition of BDMPS-Z spectra off the quark and antiquark. Therefore, in this regime the total spectrum consists of the angular ordered vacuum spectrum augmented with the BDMPS-Z emissions and, remarkably, the overall coherence of the system is not altered.

In Section 5, we proved that this leads to an exceptionally simplified picture for opaque media. The increase of the density leads to an extended window of phase space where coherence effects dominate, as  $\omega^* \rightarrow \infty$ . In effect, the emitters are completely screened by the medium to each other, i.e., “forget” about the existence of all other color charges, and radiates *as if* in vacuum. This parallels to a large extent the situation in the soft limit [20] (c.f. Appendix Appendix B). On top of that, when the total color charge of the pair is non-zero, explicitly  $C_A$  in our discussion, it will induce additional radiation at large angles which can be interpreted as radiation off the parent gluon *imagined* to be on-shell, analogously to the situation in vacuum [21].

The decomposition above parallels the jet calculus in vacuum [22, 27] and is anticipated to be the building block in future efforts of constructing a full shower picture valid for heavy-ion collisions. Regrettably, a more detailed analysis of the antenna spectrum goes beyond the scope of this first, exploratory study. We therefore postpone an exhaustive discussion and a numerical evaluation of the spectrum derived here to a forthcoming publication.

## Acknowledgements

We would like to thank Carlos Salgado for stimulating discussions. This work is supported by Ministerio de Ciencia e Innovación of Spain; by Xunta de Galicia (Consellería de Educación and Consellería de Innovación e Industria – Programa Incite); by the Spanish Consolider-Ingenio 2010 Programme CPAN; by the European Commission and in part by the Swedish Research Council (contract number 621-2010-3326).

## Appendix A. Reduction formula Eq. (7)

In this appendix we shall see how we obtain the reduction formula (7). To alleviate the notation let us consider a generic field  $A(x)$ . Then, the amplitude

for real gluon production is given by the LSZ reduction formula,

$$\mathcal{M}(\vec{k}) = \lim_{k^2 \rightarrow 0} \int d^4x e^{ik \cdot x} \square_x A(x), \quad (\text{A.1})$$

where  $x^+$  is evaluated up to some finite value which should then be sent to infinity.

Explicitly,

$$\begin{aligned} \mathcal{M}(\vec{k}) &= \lim_{k^2 \rightarrow 0} \lim_{z^+ \rightarrow +\infty} \int^{z^+} d^4x e^{ik \cdot x} (2\partial^+ \partial^- - \partial^2) A(x) \\ &= \lim_{k^2 \rightarrow 0} \lim_{z^+ \rightarrow +\infty} \left[ \int dx^- d^2\mathbf{x} e^{ik \cdot x} 2\partial^+ A(x) \Big|_{x^+ = z^+} \right. \\ &\quad \left. - ik^- \int^{z^+} dx^+ d^2\mathbf{x} e^{ik \cdot x} A(x) \Big|_{x^- = +\infty} \right. \\ &\quad \left. - k^2 \int^{z^+} d^4x e^{ik \cdot x} A(x) \right]. \end{aligned} \quad (\text{A.2})$$

The second term vanishes since the field vanishes in the limit  $x^- \rightarrow \infty$ . The remaining two terms are sensitive to the order of the limits. E.g., taking the  $z^+$  limit first leads to the standard relation

$$\mathcal{M}(\vec{k}) = \lim_{k^2 \rightarrow 0} -k^2 A(k), \quad (\text{A.3})$$

where the field is defined in momentum space. On the other hand, enforcing the on-shell condition from the outset, we end up with

$$\mathcal{M}(\vec{k}) = \lim_{x^+ \rightarrow +\infty} \int dx^- d^2\mathbf{x} e^{ik \cdot x} 2\partial_x^+ A(x), \quad (\text{A.4})$$

where all quantities are defined in coordinate space and we have specified the space-time point the derivative acts upon.

## Appendix B. The gluon spectrum in the soft limit

The dominant part of the amplitude (23) for soft gluons, i.e.,  $\omega \rightarrow 0$ , is found for  $y^+ > L$  which yields

$$\mathcal{M}_{\lambda,q}^a(\vec{k}) \Big|_{y^+ > L} = -ig e^{i\frac{p \cdot k}{p^+} L} \frac{\boldsymbol{\kappa} \cdot \boldsymbol{\epsilon}_\lambda}{x(p \cdot k)} U_p^{ab}(L, 0) Q_q^b. \quad (\text{B.1})$$

The total antenna spectrum in the soft limit thus becomes

$$\mathcal{M}_\lambda^a(\vec{k}) \Big|_{\omega \rightarrow 0} = -ig \left[ \frac{\boldsymbol{\kappa} \cdot \boldsymbol{\epsilon}_\lambda}{x(p \cdot k)} U_p^{ab}(L, 0) Q_q^b + \frac{\bar{\boldsymbol{\kappa}} \cdot \boldsymbol{\epsilon}_\lambda}{\bar{x}(\bar{p} \cdot k)} U_{\bar{p}}^{ab}(L, 0) Q_{\bar{q}}^b \right], \quad (\text{B.2})$$

which was first calculated in [20]. For the color octet antenna, taking the square of (B.2) and summing over gluon polarizations leads to the spectrum in the soft limit, given by

$$dN\Big|_{\omega\rightarrow 0} = \frac{\alpha_s}{(2\pi)^2} \left[ C_F (\mathcal{R}_q^{\text{vac}} + \mathcal{R}_{\bar{q}}^{\text{vac}} - 2(1 - \Delta_{\text{med}}) \mathcal{J}^{\text{vac}}) + C_A(1 - \Delta_{\text{med}}) \mathcal{J}^{\text{vac}} \right] \frac{d^3k}{(k^+)^3}, \quad (\text{B.3})$$

where all information about the medium resides in  $\Delta_{\text{med}}$  [20]. Note that Eq.(B.3) tends to Eq. (44) in the opaque limit, when  $\Delta_{\text{med}} \rightarrow 1$ .

## References

- [1] S. S. Adler *et al.* [ PHENIX Collaboration ], Phys. Rev. **C69** (2004) 034910.
- [2] J. Adams *et al.* [ STAR Collaboration ], Phys. Rev. Lett. **91** (2003) 172302.
- [3] K. Aamodt *et al.* [ALICE Collaboration], Phys. Lett. B **696** (2011) 30.
- [4] J. Adams *et al.* [ STAR Collaboration ], Phys. Rev. Lett. **91** (2003) 072304.
- [5] S. S. Adler *et al.* [ PHENIX Collaboration ], Phys. Rev. Lett. **97** (2006) 052301.
- [6] J. Putschke [STAR Coll.], Eur. Phys. J. C **61** (2009) 629.
- [7] S. Salur [STAR Coll.], Eur. Phys. J. C **61** (2009) 761.
- [8] Y. S. Lai [PHENIX Coll.], Nucl. Phys. A **830** (2009) 251C.
- [9] G. Aad *et al.* [Atlas Coll.], [arXiv:1011.6182 [hep-ex]];
- [10] S. Chatrchyan *et al.* [CMS Coll.], [arXiv:1102.1957 [nucl-ex]].
- [11] R. Baier, Y. L. Dokshitzer, A. H. Mueller, S. Peigne, D. Schiff, Nucl. Phys. **B483** (1997) 291.
- [12] R. Baier, Y. L. Dokshitzer, A. H. Mueller, S. Peigne, D. Schiff, Nucl. Phys. **B484** (1997) 265.
- [13] B. G. Zakharov, JETP Lett. **63** (1996) 952.
- [14] B. G. Zakharov, JETP Lett. **65** (1997) 615.
- [15] U. A. Wiedemann, M. Gyulassy, Nucl. Phys. **B560** (1999) 345.
- [16] U. A. Wiedemann, Nucl. Phys. **B582** (2000) 409.
- [17] U. A. Wiedemann, Nucl. Phys. **B588** (2000) 303.
- [18] Y. Mehtar-Tani, Phys. Rev. C **75** (2007) 034908.

- [19] Y. Mehtar-Tani, C. A. Salgado, K. Tywoniuk, Phys. Rev. Lett. **106** (2011) 122002.
- [20] Y. Mehtar-Tani, C. A. Salgado, K. Tywoniuk, [arXiv:1102.4317 [hep-ph]].
- [21] Yu. L. Dokshitzer, V. A. Khoze, A. H. Mueller and S. I. Troyan, “Basics Of Perturbative QCD,” *Gif-sur-Yvette, France: Ed. Frontieres (1991) 274 p. (Basics of).*
- [22] A. Bassetto, M. Ciafaloni, G. Marchesini, Phys. Rept. **100** (1983) 201.
- [23] A. Bassetto, M. Ciafaloni, G. Marchesini, A. H. Mueller, Nucl. Phys. **B207** (1982) 189.
- [24] A. H. Mueller, Phys. Lett. B **104** (1981) 161.
- [25] B. I. Ermolaev and V. S. Fadin, JETP Lett. **33** (1981) 269.
- [26] C. A. Salgado and U. A. Wiedemann, Phys. Rev. D **68** (2003) 014008.
- [27] K. Konishi, A. Ukawa, G. Veneziano, Nucl. Phys. **B157** (1979) 45.